INL/JOU-18-44500-Revision-0

Modeling of Cr2O3-doped UO2 as a Near-term Accident Tolerant Fuel for LWRs using the BISON Code

Giovanni Pastore, Jason Hales, Koroush Shirvan, Yifeng Che

July 2018

The INL is a U.S. Department of Energy National Laboratory
operated by Battelle Energy Alliance

INL/JOU-18-44500-Revision-0

Modeling of Cr2O3-doped UO2 as a Near-term Accident Tolerant Fuel for LWRs using the BISON Code

Giovanni Pastore, Jason Hales, Koroush Shirvan, Yifeng Che

July 2018

Idaho National Laboratory
Idaho Falls, Idaho 83415

http://www.inl.gov

Prepared for the
U.S. Department of Energy
Under DOE Idaho Operations Office
Contract DE-AC07-05ID14517, DE-AC07-05ID14517

Modeling of Cr_2O_3-doped UO_2 as a Near-term Accident Tolerant Fuel for LWRs using the BISON Code

Yifeng Che,[1] Giovanni Pastore,[2] Jason Hales,[2] Koroush Shirvan[1,*]

[1]Department of Nuclear Science and Engineering, Massachusetts Institute of Technology

[2] Fuel Modeling and Simulation, Idaho National Laboratory

*Corresponding Author

Abstract:

The near-term Accident Tolerant Fuel (ATF) concepts consist of minor modifications of the standard UO_2-Zr fuel rod materials to provide enhanced accident tolerance. Uranium dioxide fuel with chromia dopant, developed by AREVA, is of interest in view of its enhanced fission gas retention. The predictive capability of the BISON fuel performance code for chromia-doped UO_2 fuel is assessed through simulation of the Halden IFA-677.1 fuel rod experiment. A sensitivity analysis is conducted to interpret the deviation of code's predictions from the experimental data. A power ramp test is also modeled with BISON and calculations are compared to the experimental database. Finally, a large-break LOCA (LBLOCA) case is simulated with BISON, leading to an initial assessment of the enhanced safety associated with chromia-doped fuel compared to the standard UO_2 fuel in LWRs.

1 Background:

Innovative fuels that provide enhanced safety and maintain economic competitiveness with respect to the current commercial nuclear fleet have drawn worldwide attention [1]. The focus of Accident Tolerant Fuel (ATF) designs is obtaining enhanced accident tolerance while maintaining or improving the fuel performance during normal reactor operation [2]. One of the key performance-limiting factors of conventional UO_2 fuel is fission gas release (FGR) at high burnup and/or under accident conditions. During the reactor operation, gaseous fission products Xenon and Krypton are generated in the fuel pellets and partly released into the free volume of the fuel rod. The accumulation of the released fission gases in the rod free volume builds up the rod internal pressure. Meanwhile, the gap conductance degrades due to the poor conductivity of the gaseous fission products relative to the initial Helium fill gas. This leads to higher fuel temperature and higher FGR in turn. FGR is a life-limiting factor for the fuel rod, and is enhanced at extended burnup and during power ramps. In particular, substantial fission gas release occurring on a small time scale has been observed during power ramps [3][4][5]. In addition to this, the contribution of FGR to the rod inner pressure promotes cladding ballooning and burst during a loss-of-coolant accident (LOCA). Also, FGR increases cladding loading and the risk of creep-induced cladding rupture by ballooning during a reactivity-initiated accident (RIA) [6]. For these reasons, it is desirable to retain gaseous fission products within the pellets to limit the detrimental effects of FGR.

One ATF concept, currently proposed by AREVA, involves modifying the conventional UO_2 fuel with dopants (e.g. small additives), which minimizes the neutronic penalty [7]. One of the most common dopant materials is chromium oxide (Cr_2O_3) [8]. Cr_2O_3 promotes formation of larger grain sizes in uranium dioxide (UO_2) fuel. Most of the thermal-mechanical properties of the Cr_2O_3-doped fuel are fundamentally the same as the UO_2 fuels [9], with improvements in the following three aspects. (i) The Cr_2O_3-doped UO_2 fuel suppresses the release of gaseous fission products at extended burnup and during power ramps compared to the traditional UO_2 fuel. (ii) Better fission gas retention provided by the Cr_2O_3-doped fuel should enhance the accident tolerance. (iii) The Cr_2O_3-doped fuel exhibits narrower, smaller but more numerous radial cracks during the reactor operation, which is beneficial from the pellet-cladding interaction and the fuel wash-out perspective [9]. (i) and (ii) are investigated in this work, with (iii) reserved for the future work.

It has been experimentally reported that the Cr_2O_3 dopant once mixed with UO_2 can serve as an effective grain growth promoter during the sintering by increasing the grain size, up to 7 times greater than the un-doped fuel [10]. During the reactor operation, the gaseous fission products produced in the fuel matrix diffuse toward the grain boundaries where the gas atoms precipitate in the form of grain-face bubbles. Bubbles grow with inflow of gas atoms from within the grains and vacancies from the grain boundaries, contributing to fuel gaseous swelling. Bubble growth brings about bubble coalescence and inter-connection, eventually leading to release of the fraction of the gas through percolated grain boundaries to the rod free volume. Experimental observations suggest that gas release may also occur through a mechanism of grain boundary

separation due to micro-cracking, especially in transients such as power ramps [3][11]. In either case, the amount of gas being available for release at grain boundaries is determined by diffusional gas transport from within the fuel grains to grain boundaries. With a larger grain size, the diffusion distance is increased, which is expected to be associated with delayed and suppressed FGR. However, it has also been reported that the enlarged grain size is accompanied by an enhanced diffusion coefficient of the gaseous fission products in the Cr_2O_3 doped fuel, as well as a reduced grain boundary surface energy [7][12]. The higher diffusion coefficient corresponds to enhanced gas atom diffusion to grain boundaries; the reduced grain boundary surface energy corresponds to larger grain-boundary bubbles and thus favors grain boundary percolation and FGR. These effects tend to increase FGR and thus to counteract the suppressing effect of the increased average grain size. Consequently, the FGR of the Cr_2O_3-doped fuels during normal reactor operations might not be significantly suppressed compared to the conventional UO_2 fuels depending on the specific operational power maneuvering. However, during the rapid transient operations of the reactors, Cr_2O_3 doped fuels show a decisive advantage in fission gas retention compared to the un-doped fuels as the burnup builds up [13]. To investigate the performance of the Cr_2O_3-doped fuel in the reactor operation, various experimental tests have been performed in the Halden reactor (Norway) and other experimental facilities.

In this work, we perform integral fuel performance analyses with Cr_2O_3-doped fuel using BISON, a finite-element based nuclear fuel performance code developed at Idaho National Laboratory (INL). The paper is structured as follows. In Section 2, the BISON code is modified and assessed

against the integral Cr_2O_3-doped fuel rod irradiation experiment Halden IFA-677.1. In Section 3, a preliminary sensitivity study is performed to point out the uncertain nature of the FGR. In Section 4, the BISON prediction for a ramp test is conducted and compared with the AREVA database. In Section 5, a large break LOCA (LBLOCA) is modeled for both the doped and un-doped fuel showing the enhanced accident tolerance provided by the Cr_2O_3-doped fuel.

2 IFA benchmark

The IFA-677.1 test in the Halden reactor was loaded with six rods supplied by Westinghouse, Framatome ANP and GNF USA, two of which contain Cr_2O_3 and Al_2O_3 doped UO_2 pellets. In rod 1 the UO_2 pellets are doped with 900 ppm Cr_2O_3 and 200 ppm Al_2O_3, and in rod 5 the UO_2 pellets consist of 500 ppm Cr_2O_3 and 200 ppm Al_2O_3 (Table 1) [14]. The irradiation began at ~45 kW/m and decreased to ~25 kW/m when the burnup reached 30 MWd/kgUO_2. The six rods went through 6 cycles and experimental data were measured from in-pile instrumentations. The measurement uncertainties of the irradiation campaign were not reported.

Table 1. Fuel Characteristics in IFA-677.1 [14]

	Rod 1	**Rod 5**
Fuel Vendor[1]	W	W
Fuel	UO_2+Add.[2]	UO_2+Add.[2]
Cr_2O_3 content	900	500
Al_2O_3 content	200	200
Average grain size (μm)	56	45

[1]W=Westinghouse AB, Sweden

[2]Add.: Cr_2O_3 and Al_2O_3 Dopants

Rod 1 and rod 5 were both manufactured by Westinghouse with identical geometry but different dopant content. In this study, rod 1 and rod 5 are benchmarked in BISON using measured data of linear heat generation rate (LHGR), coolant inlet temperature and fast neutron flux from the Halden test. For the Cr_2O_3-doped UO_2 fuel, the grain size is 4-5 times larger than for the reference UO_2 fuel rod. BISON uses the fission gas behavior and release models from [15][16][17]. The intra-granular diffusion coefficient from Turnbull et al. [18] with a correction for the effects of intra-granular bubbles is applied to obtain an effective diffusion coefficient. For the present analyses, we multiplied the intra-granular effective diffusion coefficient by a factor of three, which is a preliminary and conservative estimation based on [7][12]. Atomistic modeling work is ongoing in the NEAMS program to obtain a better assessment of the fission gas diffusion coefficient in Cr_2O_3-doped UO_2 [19]. As for the gap conductance model in BISON, a modified Mikic-Todreas [20] model that has been adopted in FRAPCON-4.0 [21] is implemented in BISON in replacement for the built-in Ross and Stoute [22] solid-solid conductance model. Before usage as BISON input, raw experimental data histories for rod linear power, coolant inlet temperature, and fast neutron flux were condensed using the 'Fuel Rod Analysis ToolBox' program [23].

The calculated fuel centerline temperature for IFA-677.1 rod 1 and rod 5 as a function of the irradiation time are shown in Figure 1 and Figure 2 along with the experimental data from the fuel centerline thermocouple. For rod 1, BISON's prediction matches the experimental data well during the first 270-day of the test. The gap closure takes place at around 270 days, after which

BISON starts to overpredict the fuel temperature by 100-200 K, and the overprediction reaches 400 K at the end stage. For rod 5, BISON slightly under-predicts and over-estimates fuel temperature before and after gap closure. The discrepancies in rod 1 and rod 5 require further investigation. As shown in Section 3, a preliminary sensitivity analysis with a limited number of parameters indicates that inherent modeling uncertainties may explain the observed deviation to a significant extent. Also, a specific thermal conductivity model for Cr_2O_3-doped UO_2 may be necessary to improve the predictions, and will be the subject of future work. Finally, uncertainties in the temperature measurements exist and may be contributing to the discrepancies. Given that the over-prediction is observed after gap closure, further investigation of the gap conductance model with specific reference to behavior during pellet-cladding contact is of special interest.

In Figure 3 and Figure 4, the calculated FGR as a function of the fuel rod average burnup is compared to the experimental data inferred from the on-line rod inner pressure measurements. Note that rod 1 has been reported with leakage during transport to the PIE hot cells, thus the puncture data is only plotted for rod 5 in Figure 4 [24]. The observed FGR for rod 1 and rod 5 are in good agreement with the measured data. However, the large uncertainty of the FGR calculation is well known, with deviations of at least a factor of 2 being expected in view of the inherent modeling uncertainties [16]. A sensitivity analysis is conducted and presented in the next section that investigates the uncertainties in both the temperature and FGR predictions for the analysis of the IFA-677.1 test.

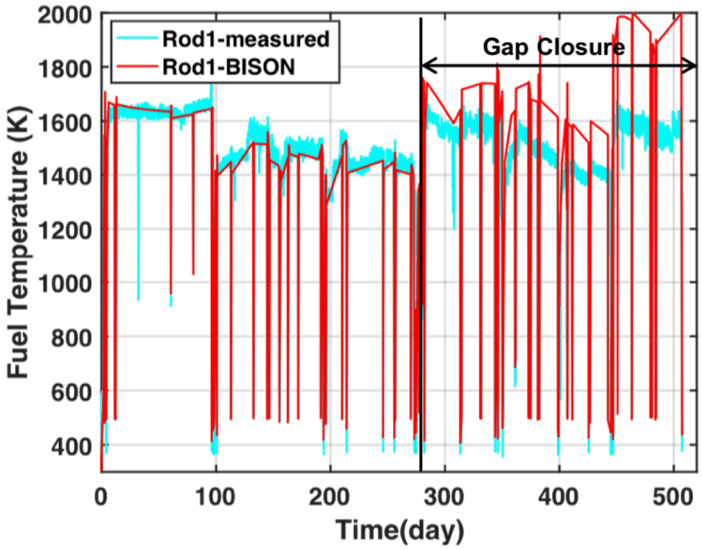

Figure 1. Simulated fuel centerline temperature in BISON vs. thermocouple data for IFA-677.1 rod 1. A modified Mikic-Todreas [20] model (used in FRAPCON-4.0) for contact gap conductance is used in the simulation.

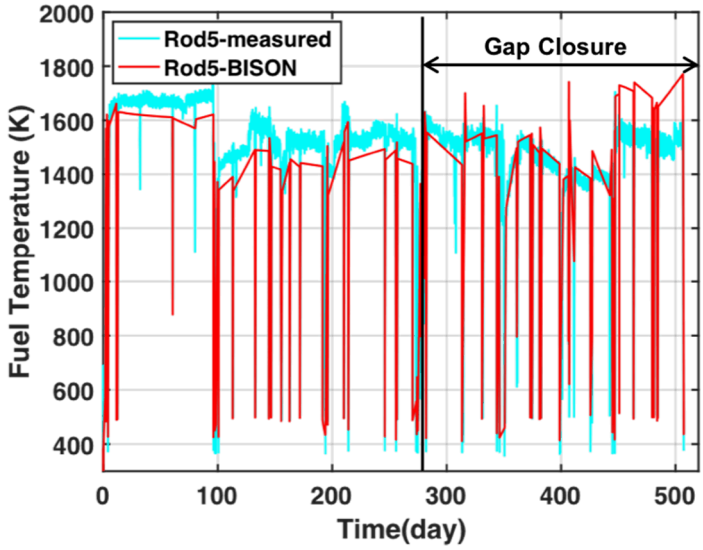

Figure 2. Simulated fuel centerline temperature in BISON vs. thermocouple data for IFA-677.1 rod 5. A modified Mikic-Todreas [20] model (used in FRAPCON-4.0) for contact gap conductance is used in the simulation.

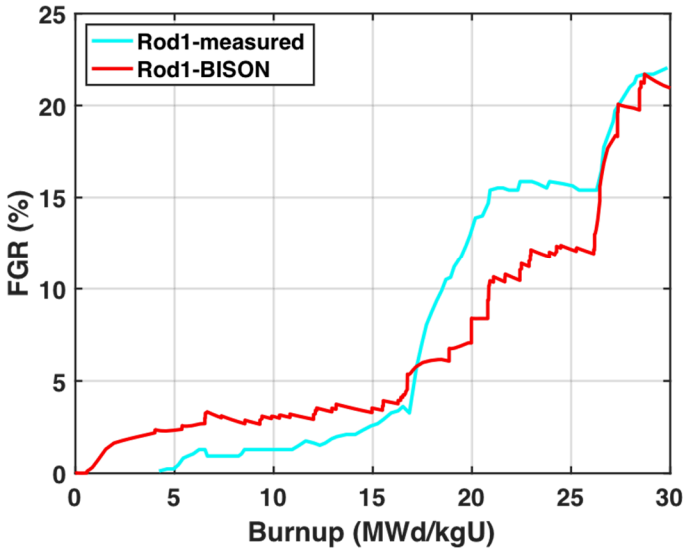

Figure 3. Simulated FGR vs. data inferred from the rod inner pressure measurements for IFA-677.1 rod 1.

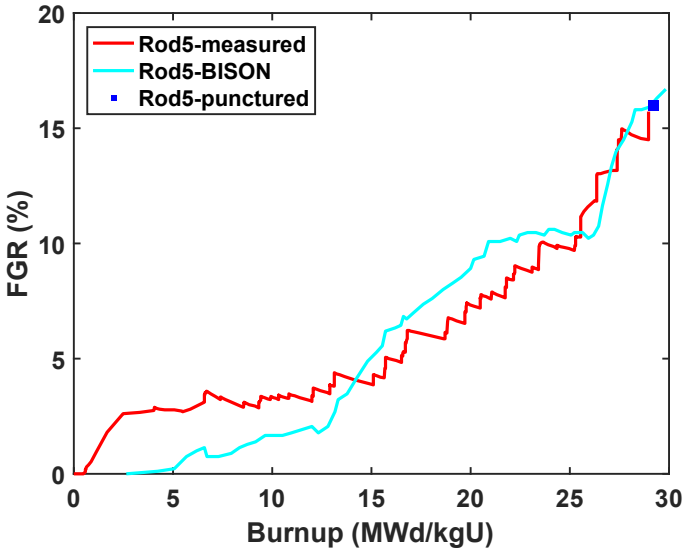

Figure 4. Simulated FGR, data inferred from the rod inner pressure measurements and puncture data for IFA-677.1 rod 5.

3 Sensitivity study of the IFA-677.1 simulation

The production and release of gaseous fission products in reactor operation have complex feedback to the thermo-mechanical behavior of the pellets and cladding. The prediction of fission gas release involves large uncertainty that not only arises from simplifying the complex physical processes into a model, but also from the uncertainties in the internal parameters of the fission gas model. Indeed, several parameters involved in fission gas behavior modeling (e.g. local grain size, diffusion coefficient, etc.) are prone to large uncertainties [16]. As shown in the previous section, the BISON code successfully predicts the fuel temperature before pellet-cladding mechanical interaction (PCMI) for rod 1 and rod 5 in IFA-677.1 test. After the gap closure, a more conservative calculation of the fuel temperature is observed while the calculated FGR matches well with the experiment. Note that an over-prediction in the fuel temperature is rather expected to lead to an over-prediction of FGR, nevertheless, uncertainties may explain such behavior. This motivates performing a sensitivity analysis to quantify uncertainties in the code predictions and compare the calculated uncertainties to the deviation of FGR in the IFA-677 case. The sources of input uncertainties in the BISON modeling contributing to the deviation of FGR can be broken into three categories, the operation uncertainties (e.g. power), manufacturing uncertainties (e.g. rod geometry) and modeling uncertainties (e.g. internal parameters in the fission gas models) [25]. A preliminary sensitivity analysis is performed in this section considering the operational uncertainties and modeling uncertainties that are expected to have the most significant impact on code predictions, based on previous sensitivity studies from the

literature [16][26][27]. For simplicity, the sensitivity analysis is only performed and shown for rod 1 in IFA-677.1 test.

The selected input parameters with the relative uncertainties and reference values are listed in Table 2. Either normal or log-normal distributions are assumed. The uncertainty of the linear heat generation rate is estimated to be $\pm 5\%$ with a 95% confidence interval [26][27]. The Cr_2O_3 dopant is expected to affect fuel densification. Pending more precise indications, an uncertain range of $\pm 20\%$ is adopted in this analysis. This range is based on author's own judgement, and is equal to the uncertainty in fuel swelling considered in [27]. The fuel temperature has been observed to be very sensitive to gas-gap conductance and solid-solid contact gap conductance in the previous studies with BISON. In this work, an uncertainty range of $\pm 50\%$ is applied to both the gas conductivity term and the fuel-cladding contact term in the gap conductance model. This range is the same applied in [26], although only the gas conductivity term was considered there. The fuel thermal conductivity is varied in the commonly accepted range of $\pm 10\%$ [27]. The inherent uncertainties in the fission gas behavior model are also considered. In particular, based on [16], we consider as important uncertain parameters the effective intra-granular diffusion coefficient, the intra-granular bubble resolution parameter, the grain-boundary diffusion coefficient of vacancies and the grain size. Uncertainty ranges for these are also based on [16].

DAKOTA (Design Analysis Kit for Optimization and Terascale Applications), an uncertainty quantification and sensitivity analysis toolkit developed by Sandia National Laboratory [28], is interfaced with BISON and used to perform the sensitivity analysis in this work. The Latin

Hypercube sampling (LHS) method is used for sampling the uncertain input parameters for the sensitivity analysis. In particular, each uncertain input parameter is sampled 20 times, and 180 samplings are performed in total. Considered that the simulation time in BISON for a single IFA-677 case takes approximately 4 hours, the real measured data in the Halden test (which was used as input in the benchmark) is smoothened to facilitate the sampling process while minimizing an introduction of any model bias.

Figure 5 shows the time-dependent sensitivity analysis of fuel centerline temperature for the BISON simulation of IFA-677.1 rod 1, including mean value and $\pm\sigma$ uncertainty range. Before PCMI, the predicted fuel temperature in BISON is well within the $\pm\sigma$ range (~200 K), and the deviation becomes larger after gap closure. The uncertainty range of the fuel temperature becomes larger after gap closure (~500 K) due to the inclusion of the uncertainty in the contact gap conductance. Results indicate that the considered inherent modeling uncertainties may explain the overestimation of temperature in this region to a significant extent. Note that only a subset of the uncertain parameters that affect fuel temperature is considered in this analysis. Furthermore, the $\pm\sigma$ uncertainty range illustrated in Figure 5 corresponds to ~68% confidence interval, while a higher confidence interval (e.g., 95%, or $\pm 2\sigma$) would correspond to a wider band. Figure 6 presents the uncertain range of the fission gas release as a function of burnup. The mean value of FGR is shown to be in relatively good agreement with the experimental data. Therefore, the adopted model settings for the benchmark is considered to be sufficient for the assessment of the Cr_2O_3-doped fuel in the next sections. In Figure 6 the mean value of the fission gas release is slightly larger than the previous result presented in Section 2. The reason is that the log-normal distribution of the intra-granular diffusion coefficient, intra-granular resolution

parameter and grain-boundary diffusion coefficient is not symmetrically distributed with respect to the reference value. The uncertainty of FGR almost reaches 30% at the burnup of ~30 MWd/kgU, which further proves that the FGR is prone to large uncertainty in the fuel performance analysis.

Table 2. Selected parameters and uncertainty ranges used in the sensitivity analysis for IFA-677.1 rod 1

Parameter	Reference value	Uncertainty Range	σ	Distribution
Linear power	Input power	$\pm$5% [27]	0.025	Normal
Total densification	9×10^{-4}	$\pm$20%	9×10^{-5}	Normal
Gas gap conductance	[22]	$\pm$50%	0.25	Normal
Contact gap conductance	[22]	$\pm$50%	2.5	Normal
Fuel thermal conductivity	NFIR model	$\pm$10% [27]	0.05	Normal
Grain radius	28 μm	$\pm$60% [16]	0.3	Normal
Intra-granular diffusion coefficient	[29][30]	Factor of 100 [16]	0.5	Log-Normal
Intra-granular resolution parameter	[29][30]	Factor of 100 [16]	0.5	Log-Normal
Grain-boundary diffusion coefficient	[29][30]	Factor of 100 [16]	0.5	Log-Normal

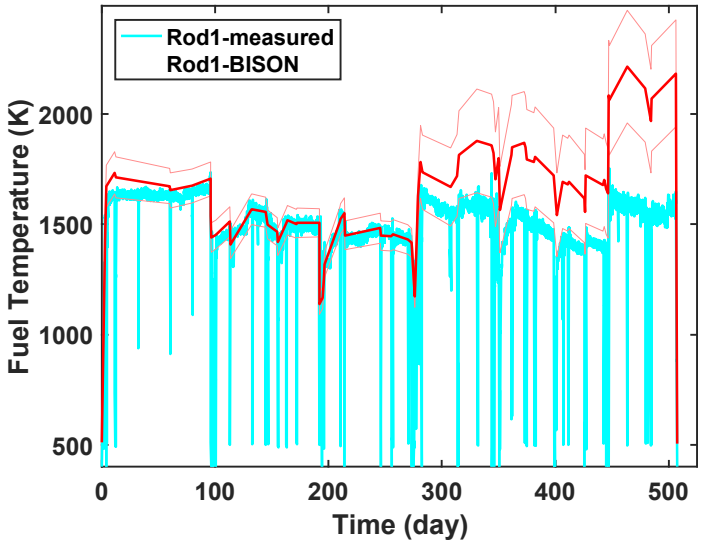

Figure 5. Time-dependent sensitivity analysis of fuel centerline temperature for the BISON simulation of IFA-677.1 rod 1 (The solid red line is the mean value of the simulated fuel temperature. The light red band denotes the $\pm\sigma$ uncertain range. The solid line in cyan is the real measured temperature from the Halden test).

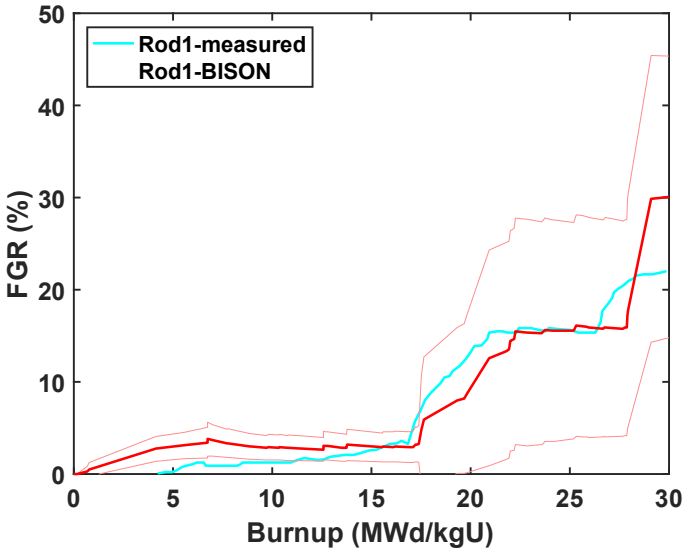

Figure 6. Time-dependent sensitivity analysis of fission gas release for the BISON simulation of IFA-677.1 rod 1 (The solid red line is the mean value of the FGR. The light red band is the $\pm\sigma$ uncertainty range. The solid line in cyan is the experimental FGR inferred from the rod pressure measurements).

4 BISON simulation of ramp tests and comparisons to the AREVA database

Ramp tests of 0.16 wt.% Cr_2O_3-doped fuel (i.e. 1600 ppm Cr_2O_3) have been carried out by AREVA under various operating conditions that cover both PWR (in OSIRIS test reactor at CEA, France or in Halden test reactor, Norway) and BWR (in Halden test reactor, Norway) environments [13]. The in-pile experiments show that the Cr_2O_3-doped fuel provides the desired enhanced fission gas retention during the ramp tests, as shown in Figure 7, which is reproduced from [13]. The AREVA tests also showed better pellet mechanical compliance (i.e. PCMI). The ramp testing of standard UO_2 fuel under PWR conditions leads to enhanced increase of the fission gas release as the ramp test terminal power level increases. The substantial release of fission gas can lead to the build-up of rod internal pressure. High plenum pressures can

contribute to fuel rod failure and the subsequent release of radioactive nuclides into the reactor primary system. On the contrary, the released fission gas in Cr_2O_3-doped UO_2 fuel only increases linearly as the ramp terminal increases. A power ramp is considered to be a limiting LWR operating condition and involves increased FGR due to burst release as well as fuel thermal expansion and swelling potentially leading to cladding failure due to pellet-cladding interaction (PCI) [31].

Due to the limited information of the AREVA database, the ramp test in BISON is performed based on an optimal case designed for an idealized French commercial pressurized water reactor provided by AREVA [32], with the rod design specified in Table 3. A simplified power history is adopted in this BISON simulation. The fuel is first irradiated at 12.5 kW/m until a burnup of 20 MWd/kgU after which the power goes down to zero to mimic reactor shut-down and rod transfer between reactors. Then the fuel is pre-conditioned to be constant at 12.5 kW/m, and ramped to different terminal levels of 38, 40, 42, 45, 48, 50, and 53 kW/m respectively with a ramping rate of ~1.67 W/s. The fuel rod is then maintained at the ramped power terminal for 12 hours [13], and the LHGR for the power ramping is shown in Figure 7. The peaking factors are assumed to be of a chopped cosine-shape with the peak-to-average ratio being ~1.2. The standard UO_2 fuel and the Cr_2O_3-doped UO_2 fuel are modeled in BISON under the aforementioned operating conditions. For the Cr_2O_3-doped UO_2 fuel, the effect of enlarged grain size and enhanced diffusion coefficient are accommodated in the grain growth model and the fission gas release model. An initial grain diameter of 56 μm is used for the Cr_2O_3-doped fuel, and correspondingly a grain diameter of 15.6 μm is used for the fresh UO_2 fuel.

Table 3. Fuel rod design specifications

Fuel Rod			**Pellet Dishing**		
Fuel stack length	3.65	m	Dish diameter	6.0	mm
Nominal plenum volume	8.04	cm^3	Dish depth	0.31	mm
Number of pellets per rod	275	/	Chamfer width	0.5425	mm
Fill gas composition	He	/	Chamfer depth	0.27	mm
Fill gas pressure	1.6	MPa			
Fuel			**Cladding**		
Material	UO_2	/	Material	Zr-4 (stress-relieved)	
Enrichment	4.5	%	Outer diameter	9.5	mm
Density	95	%	Inner diameter	8.25	mm
Outer Diameter	8.085	mm	Wall thickness	0.625	mm
Grain radius	15.6	μm			

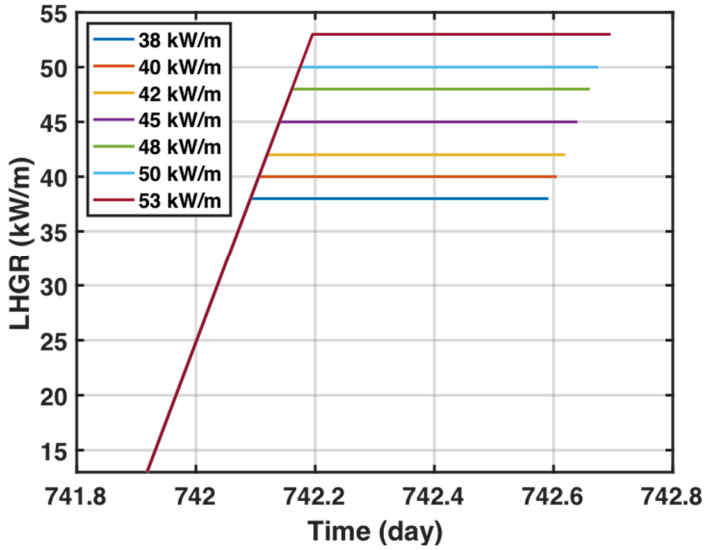

Figure 7. Linear heat generation rate (LHGR) used in BISON for the ramp tests.

Solid lines in Figure 8 show the comparison of FGR between the conventional UO_2 fuel and Cr_2O_3-doped UO_2 fuel in BISON during ramp tests for the modeled PWR rod. In the standard UO_2 fuel, the FGR increases more rapidly with the ramp terminal power level. A slower growing trend of the fission gas release is observed for the Cr_2O_3-doped UO_2 fuel. Thus, it appears that the larger grain size effectively suppresses the FGR for these conditions, at least above ramp terminal power levels of ~40 kW/m. However, for lower ramp power terminal levels, the difference of simulated FGR between the doped fuel and standard UO_2 fuel becomes not significant. Note that grain size affects the fission gas behavior both by increasing the average diffusion distance for gas atoms generated in the grains and by reducing the grain surface to volume ratio, hence, the capacity of the grain faces to store fission gas. This second effect indeed promotes FGR. Both effects are naturally considered in the BISON physics-based fission gas model. Additionally, fission gas diffusivity is higher in doped fuel. According to the present

results and to the AREVA data in Figure 8, the effects that tend to suppress FGR with a higher grain size dominate at the higher ramp terminal levels. This also appears to be consistent with the results of the sensitivity analysis for the effect of grain size on FGR at various power levels presented in [16]. Comparing the BISON results to the AREVA database (Figure 8), the FGR for the standard UO_2 and doped-UO_2 are in encouraging agreement, also in view of the uncertainties discussed in Section 3.

The calculated maximum fuel-cladding contact pressures for the standard UO_2 fuel and the Cr_2O_3-doped UO_2 fuel at different ramp terminal levels are compared in Figure 9. The contact pressure for the Cr_2O_3-doped UO_2 fuel is lower upon ramped power. Since more fission gases are retained in the grains rather than accumulating at grain boundaries in the form of bubbles, less volumetric swelling takes place in the Cr_2O_3-doped UO_2 fuel resulting in less forceful closure of the fuel-cladding gap. Lower interfacial pressure is beneficial from the perspective of potential rod failure due to PCI. Cr_2O_3-doped UO_2 fuel has been observed to present more numerous but smaller cracks around the pellet rim to mitigate PCMI. An increased number of cracks is expected to further reduce the elastic modulus of the fuel pellet, and less stiffness in the fuel will relieve the interfacial pressure upon gap closure. This work does not take into account such change in the fuel crack model for the doped fuel at this time, which is reserved as future work.

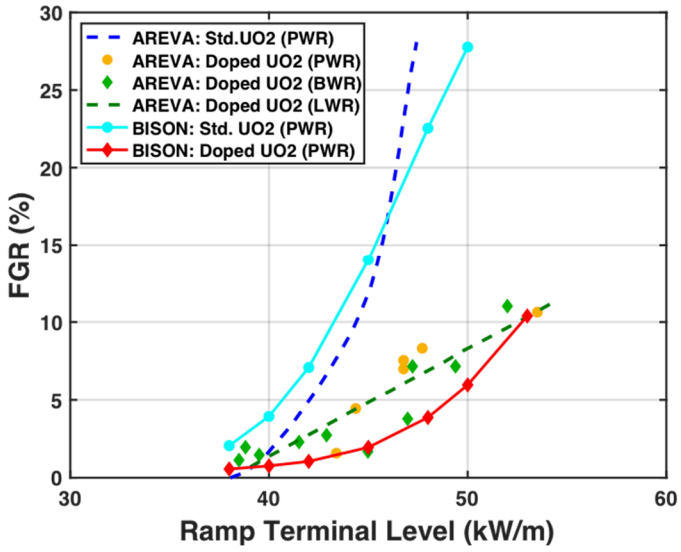

Figure 8. Fission gas release of Cr_2O_3-doped UO_2 fuel in the AREVA database (reproduced from [13]) and BISON simulations.

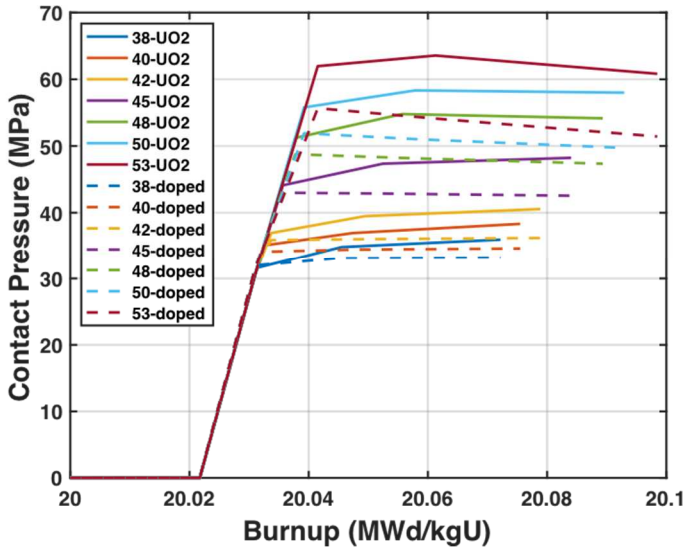

Figure 9. Contact pressure of the standard UO_2 fuel versus the Cr_2O_3-doped UO_2 fuel from the BISON simulations.

5 LBLOCA performance

The main goal of ATF designs is to improve the fuel accident response. Large-break loss of coolant accident (LBLOCA) is one of the limiting scenarios that lead to rapid loss of coolant. During a LOCA, the post-scram decay heat in the reactor core boils off the coolant, leading to a sharp increase in the fuel temperature and accelerated cladding oxidation. The high temperature results in degradation of the cladding mechanical strength which causes fuel rod ballooning, potentially compromising the coolable geometry. Fuel rod burst is expected during the heatup process, releasing the inventory of radioactive gaseous fission products into the reactor core and contaminating the primary loop [32]. To mitigate the consequence of a LBLOCA, the following fuel rod performance characteristics are desirable.

(i). Reduced ballooning in the Zr-4 cladding.

When exposed to high temperature, the cladding is subject to degradation in mechanical properties and large creep deformation under the inner gas pressure, leading to ballooning. The large deformation in the cladding can block the coolant channel, further deteriorating heat removal from the fuel rod (i.e. loss of coolable geometry). For this reason, a reduced ballooning is desired in case of a LOCA to improve resistance to burst failure and reduce the fuel rod blockage in the coolant channel.

(ii). Longer survival time.

Improving coping time in response to various accident scenarios as well as maintaining satisfying operational performance during normal conditions is a major emphasis of ATFs. It is

important to delay the fuel rupture during LOCA to gain more response time for the emergency core cooling systems to function and reflood the reactor core.

In this work, the doped fuel response during LBLOCA is simulated using BISON. To simulate the response of Cr_2O_3-doped UO_2 fuel during a limiting LBLOCA condition, the traditional UO_2 fuel and Cr_2O_3-doped fuel are initially irradiated under a constant LHGR of 21 kW/m for 962 days up to a burnup of ~38 MWd/kgU with the presence of two reactor shutdowns (each shutdown period lasts for 25 days) before the initiation of LBLOCA. The LOCA scenario is first simulated in the system code RELAP5 [33], and the obtained LHGR, coolant pressure and cladding outer surface temperature are used as BISON input. Figure 10 shows the normalized reactor power and coolant pressure upon the start of the LOCA, and Figure 11 illustrates the temperature at different elevations of the cladding outer surface during the LOCA progression. A chopped cosine peaking factor is also obtained from the RELAP5 output with a peak-to-average of ~1.5. The fresh fuel in the LOCA condition is of less interest in this work because the suppressed FGR cannot be observed without the accumulation of fission products. For this reason, the fresh fuel is first simulated under a normal condition in order to accumulate significant burnup. A LOCA condition follows subsequently until the fuel rods rupture.

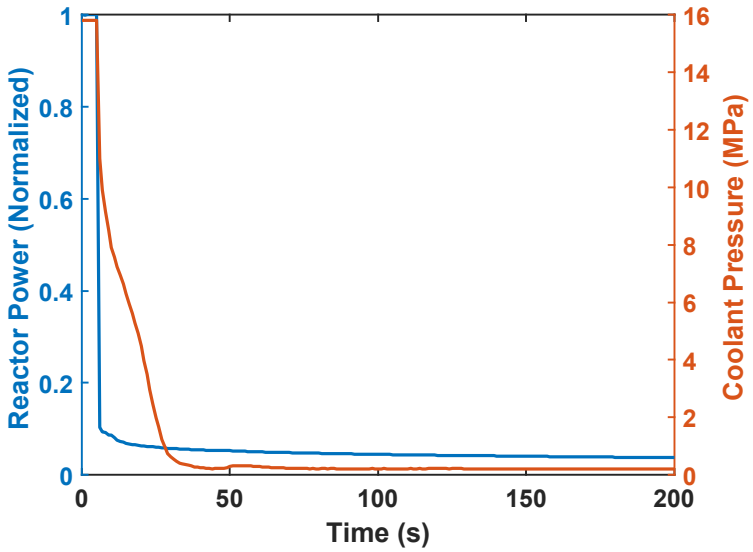

Figure 10. Normalized reactor power and coolant pressure upon the start of LOCA used as BISON input.

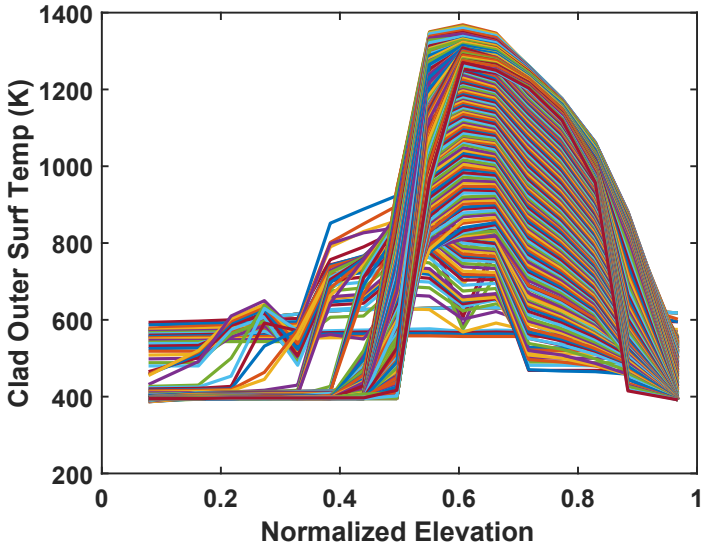

Figure 11. Cladding outer surface temperature as a function of the normalized fuel elevation, used as BISON input. Different curves correspond to different times during the simulation.

The fuel performance features depend on specific operating conditions and accident scenarios. During normal operation (Figure 12 a), the FGR goes up to 17% and plenum pressure accumulates to ~14 MPa in the standard UO_2 fuel, while the FGR and plenum pressure are suppressed to ~8% and ~8 MPa, respectively, in the Cr_2O_3-doped fuel. In the subsequent LOCA (Figure 12 b), the FGR nearly remains constant, and the plenum pressure is 2 MPa lower in the doped fuel than in the standard fuel. In this specific case, the conventional UO_2 fuel rod survives for ~108 seconds, while the rupture of the doped fuel is delayed by 10 seconds compared to un-doped UO_2 fuel, providing slightly longer coping time. At the time of the fuel rod failure, a lower amount of radioactive gas would be released into the coolant channel by using the Cr_2O_3-doped fuel because more radioactive fission products are retained in the fuel pellets. Also, the ballooning effect is less severe in the Cr_2O_3-doped fuel rod, mitigating concerns regarding coolant blockage. Figure 13 shows the ballooning effect of the cladding at the time when the fuel rod bursts (bursted elements are in red). The cladding ballooning is more pronounced for the UO_2 fuel (Figure 13 a) than the Cr_2O_3-doped UO_2 fuel (Figure 13 b). This is associated with the lower FGR and consequently lower rod inner pressure. Figure 14 compares the cladding deformation at the time of the fuel rod failure. The maximum radial displacement of the cladding in the standard UO_2 fuel is almost twice that of the doped fuel. The more significant ballooning in the standard UO_2 fuel narrows the coolant channel hence further deteriorating the heat removal capability during the LOCA. Overall, these initial simulations indicate that the Cr_2O_3-doped UO_2 fuel enhances the accident tolerance by delaying the fuel rod failure, reducing the amount of released radioactivity upon fuel rod rupture as well as mitigating the fuel rod ballooning effect, hence reducing potential blockage in the coolant channel.

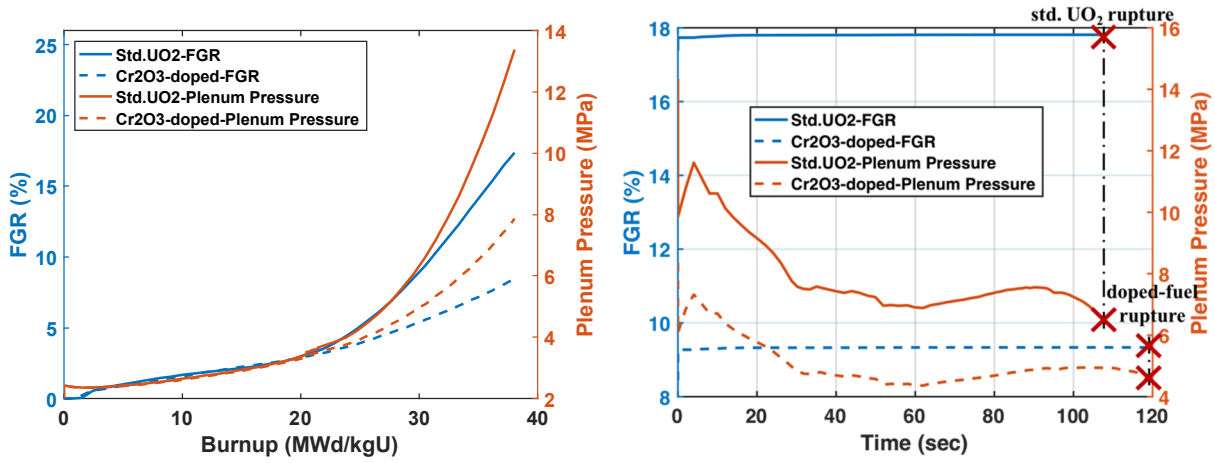

(a). (b).

Figure 12. BISON results of FGR and plenum pressure for the standard UO_2 fuel and Cr_2O_3-doped fuel. (a). Normal operation at constant power of 21 kW/m with two shutdown periods up to 38 MWd/kgU. (b). Subsequent LBLOCA with input parameters specified in Figure 10 and Figure 11.

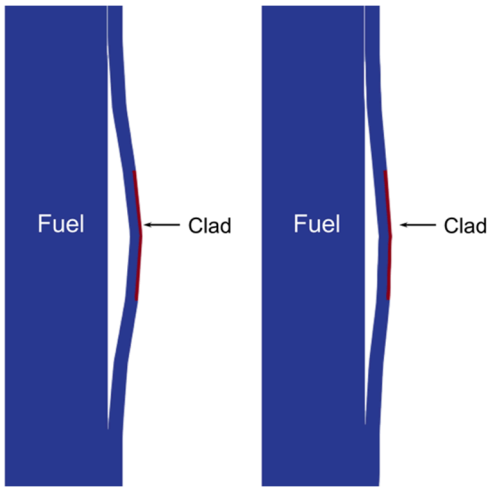

(a). (b).

Figure 13. BISON results of cladding ballooning for standard UO_2 and Cr_2O_3-doped UO_2 fuel at the time of fuel rupture in BISON. (a). Standard UO_2 fuel. (b). Cr_2O_3-doped UO_2 fuel.

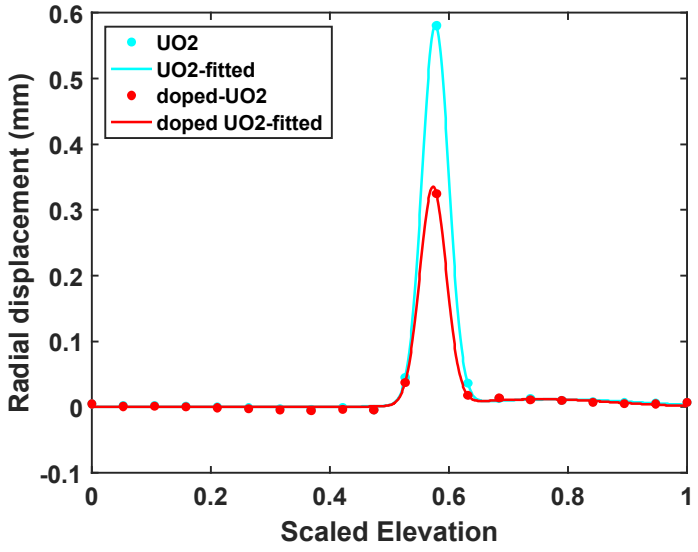

Figure 14. Radial displacement of the cladding when the fuel rod bursts for standard UO_2 fuel and Cr_2O_3-doped UO_2 fuel for the BISON simulation.

6 Conclusions

In this work, fuel rod performance calculations for large-grained Cr_2O_3-doped UO_2 fuel were performed with the BISON fuel performance code. The different grain size and fission gas diffusivity in doped fuel compared to standard UO_2 were considered in the simulations. First, BISON was assessed against the Halden IFA-677.1 experiment, which provided a benchmark case for Cr_2O_3-doped fuel. Although predictions of fuel temperature and FGR were overall satisfactory, some discrepancies were observed, in particular in the calculated fuel temperature after fuel-cladding gap closure. The inherent uncertainty in the fuel performance modeling was investigated with a sensitivity analysis, showing the impact of the uncertainties in some modeling parameters on the results. It was concluded that the considered inherent modeling uncertainties may explain the observed discrepancies to a significant extent . Then, power ramp

tests of Cr_2O_3-doped UO_2 fuel rods were simulated with BISON, showing a satisfactory agreement of FGR predictions with the AREVA experimental database. Simulations captured the suppression of FGR relative to standard fuel, and the trend of a lower increase of FGR with increasing ramp terminal power level, confirming this advantage of Cr_2O_3-doped fuel over the conventional UO_2 fuel during power ramps. Finally, simulations were performed of fuel behavior under accident conditions of a LBLOCA. BISON predictions indicated that the fuel rod with Cr_2O_3-doped UO_2 was subject to a lower FGR and as a consequence, a reduced ballooning, less radioactive gas release upon fuel rod failure, and delayed fuel rod rupture compared to the fuel rod with standard UO_2. Investigation of the difference in fuel cracking and its implication on PCMI and fuel washout behavior post-burst is reserved for future work.

Acknowledgments

Work for this paper was supported by the MIT-led DOE NEUP IRP grant (DE-NE0008416). This work was also partly supported by the Nuclear Energy Advanced Modeling and Simulation (NEAMS) program through first author's internship at INL.

The authors also gratefully acknowledge Chris Lewis and the IRP AREVA team for discussion regarding doped fuel performance, and Kyle Gamble (INL) for discussion about the sensitivity analysis.

Bibliography

[1]. Bragg-Sitton, S. (2014). Development of advanced accident-tolerant fuels for commercial LWRs. Nuclear News, 57(3), 83.

[2]. Koo, Y. H., Yang, J. H., Park, J. Y., Kim, K. S., Kim, H. G., Kim, D. J., ... & Song, K. W. (2014). KAERI's development of LWR accident-tolerant fuel. Nuclear Technology, 186(2), 295-304.

[3]. Hastings, I. J., Smith, A. D., Fehrenbach, P. J., & Carter, T. J. (1986). Fission gas release from power-ramped UO2 fuel. Journal of Nuclear Materials, 139(2), 106-112.

[4]. Walker, C. T., Knappik, P., & Mogensen, M. (1988). Concerning the development of grain face bubbles and fission gas release in UO2 fuel. Journal of Nuclear Materials, 160(1), 10-23.

[5]. Tech. Rep. RISØ-FGP3-AN3, The Third Risø Fission Gas Project: Bump Test AN3 (CB8-2R), OECD Halden Reactor Project, 1990.

[6]. Desquines, J., Koss, D. A., Motta, A. T., Cazalis, B., & Petit, M. (2011). The issue of stress state during mechanical tests to assess cladding performance during a reactivity-initiated accident (RIA). Journal of Nuclear Materials, 412(2), 250-267.

[7]. Killeen, J. C. (1980). Fission gas release and swelling in UO2 doped with Cr2O3. Journal of Nuclear Materials, 88(2-3), 177-184.

[8]. Mieszczynski, C. (2014). Atomic scale structural modifications in irradiated nuclear fuels (Doctoral dissertation, Paris 11).

[9]. Incorporation of Chromia-Doped Fuel Properties in AREVA Approved Methods, Topical Report, ANP-10340NP, Revision 0.

[10]. Volkov, B., Tverberg, T., & McGrath, M. (2014). Experimental investigations of additives on irradiation performances of oxide fuel.

[11]. Une, K., & Kashibe, S. (1990). Fission gas release during post irradiation annealing of BWR fuels. Journal of Nuclear Science and Technology, 27(11), 1002-1016.

[12]. Kashibe, S., & Une, K. (1998). Effect of additives (Cr_2O_3, Al_2O_3, SiO_2, MgO) on diffusional release of 133Xe from UO_2 fuels. Journal of nuclear materials, 254(2), 234-242.

[13]. C. Delafoy, V. I. Arimescu, R. M. Hengstler-Eger, H. Landskron, A. Moeckel. AREVA Cr_2O_3-doped fuel: Increase in operational flexibility and licensing margins. Top Fuel 2015.

[14]. Radomir Josek (2008). The high initial rating test IFA-677.1: Final report on in-pile results. Technical report HWR-872, Halden Reactor Project.

[15]. Pastore, G., Luzzi, L., Di Marcello, V., & Van Uffelen, P. (2013). Physics-based modelling of fission gas swelling and release in UO 2 applied to integral fuel rod analysis. Nuclear Engineering and Design, 256, 75-86.

[16]. Pastore, G., Swiler, L. P., Hales, J. D., Novascone, S. R., Perez, D. M., Spencer, B. W., ... & Williamson, R. L. (2015). Uncertainty and sensitivity analysis of fission gas behavior in engineering-scale fuel modeling. Journal of Nuclear Materials, 456, 398-408.

[17]. Barani, T., Bruschi, E., Pizzocri, D., Pastore, G., Van Uffelen, P., Williamson, R. L., & Luzzi, L. (2017). Analysis of transient fission gas behaviour in oxide fuel using BISON and TRANSURANUS. Journal of Nuclear Materials, 486, 96-110.

[18]. Turnbull, J. A., Friskney, C. A., Findlay, J. R., Johnson, F. A., & Walter, A. J. (1982). The diffusion coefficients of gaseous and volatile species during the irradiation of uranium dioxide. Journal of Nuclear Materials, 107(2-3), 168-184.

[19]. D.A. Andersson, M. Cooper, C. Matthews, R. Perriot, X.-Y. Liu, C.R. Stanek, Atomistic simulations of point defect behavior in nuclear fuels. Transactions of the ANS Annual Meeting, Philadelphia, PA, USA, June 17-21, 2018.

[20]. Jacobs, G., & Todreas, N. (1973). Thermal contact conductance in reactor fuel elements. Nuclear science and engineering, 50(3), 283-290.

[21]. Geelhood, K. J., Luscher, W. G., & Beyer, C. E. (2011). FRAPCON-4.0: A Computer Code for the Calculation of Steady-State. Thermal-Mechanical Behavior of Oxide Fuel Rods for High Burnup (NUREG/CR-7022, Volume 1, PNNL-19418, Volume 1), published March.

[22]. A. M. Ross and R. L. Stoute. Heat transfer coefficient between UO2 and Zircaloy-2. Technical Report AECL-1552, Atomic Energy of Canada Limited, 1962.

[23]. K. Lassmann, A. Schubert, J. van de Laar, P. Van Uffelen. The 'Fuel Rod Analysis ToolBox': a general program for preparing the input of a fuel rod performance code. Ann. Nucl. Energy 81, 332–335, 2015

[24]. Hakon K. Jenssen (2010). PIE report on six UO2 fuel rods irradiated in IFA-677 high initial rating test. Technical report HWR-968, Halden Reactor Project.

[25]. Kyle A. Gamble, Laura P. Swiler. Uncertainty Quantification and Sensitivity Analysis Applications to Fuel Performance Modeling. Top Fuel 2016.

[26]. Bouloré, A., Struzik, C., & Gaudier, F. (2012). Uncertainty and sensitivity analysis of the nuclear fuel thermal behavior. Nuclear Engineering and Design, 253, 200-210.

[27]. Ikonen, T., & Tulkki, V. (2014). The importance of input interactions in the uncertainty and sensitivity analysis of nuclear fuel behavior. Nuclear Engineering and Design, 275, 229-241.

[28]. B.M. Adams, K.R. Dalbey, M.S. Eldred, L.P. Swiler, W.J. Bohnhoff, J.P. Eddy, D.M. Vigil, P.D. Hough, S. Lefantzi, DAKOTA: A Multilevel Parallel Object-oriented Framework for Design Optimization, Parameter Estimation, Uncertainty Quantification, and Sensitivity Analysis. Version 5.2 User's Manual, Tech. Rep. SAND2010-2183, 2011

[29]. White, R. J., & Tucker, M. O. (1983). A new fission-gas release model. Journal of Nuclear Materials, 118(1), 1-38.

[30]. Speight, M. V. (1969). A calculation on the migration of fission gas in material exhibiting precipitation and re-solution of gas atoms under irradiation. Nuclear Science and Engineering, 37(2), 180-185.

[31]. Cox, B. (1990). Pellet-clad interaction (PCI) failures of zirconium alloy fuel cladding—a review. Journal of Nuclear Materials, 172(3), 249-292.

[32]. Perez, D. M., Williamson, R. L., Novascone, S. R., Pastore, G., Hales, J. D., & Spencer, B. W. (2013). Assessment of BISON: A nuclear fuel performance analysis code. Tech. Rep. INL/MIS-13-30314, Idaho National Laboratory.

[33]. Feng, D., Hejzlar, P., & Kazimi, M. S. (2007). Thermal-hydraulic design of high-power-density annular fuel in PWRs. Nuclear Technology, 160(1), 16-44.